Strange quark matter in compact stars

Yu. L. Vartanyan,[*]   **G. S. Hajyan**,[†]   **G. B. Alaverdyan**,[‡]
A. K. Grigoryan, A. R. Harutyunyan, A. G. Alaverdyan, H. A. Shahinyan

Yerevan State University, Research Laboratory of Extreme States of Matter and their
Astrophysical Manifestations, 1 Alex Manoogian St., Yerevan 0025, Armenia

This paper is based on three reports by the first three authors of this contribution at the conference *"The Modern Physics of Compact Stars and Relativistic Gravity 2015"*. These three reports were devoted to strange quark matter in compact stars, which is studied in the framework of MIT bag model quark matter. In the first part of the presented work, sets of values of the MIT bag model constants are determined, which if used in the equation of state for SQM yield a maximal mass M_{max} of the equilibrium quark configurations exceeding the recently accurately determined mass $2.01 M_\odot$ for the radio pulsar PSR $J0348 + 0432$ in a binary with a white dwarf. Meanwhile, we find that if the quark-gluon interaction constant α_c is limited to values $\alpha_c < 0.6$, then all three pulsars with the most accurately measured masses $(M/M_\odot = 1.44, 1.97$ and $2.01)$ may be candidates for strange stars. In the second part of this paper, the maximum masses for hybrid stars are determined for various combinations of the equation of state of baryonic matter with the equation of state of strange quark matter. It is shown that in for combinations considered, the maximum mass of a hybrid star does not reach the value $2.01 M_\odot$. In the third part of this work, the dependence of the radius of the strange dwarfs on their mass is investigated for different chemical compositions of the outer shell. According to these results, on the mass-radius plane, the regions of existence of white dwarfs and strange dwarfs are overlapped. It is shown that white dwarfs G234-44, G181-135B and EG50 are possible candidates for strange dwarfs.

[*]Speaker, E-mail: yuvartanyan@ysu.am, presentation: *Pulsars with more exactly measured masses as possible candidates of strange stars.*

[†]Speaker, E-mail: gevorg.hajyan@gmail.com, presentation: *Mass-radius relation of white and strange dwarfs.*

[‡]Speaker, E-mail: galaverdyan@ysu.am, presentation: *Scalar-isovector channel of the nucleon-nucleon interaction in the RMF theory and massive compact stars.*

1. Introduction

Functional relationships between integral parameters of compact stars (mass, radius, moment of inertia, red shift, etc.) and the equation of state (EOS) allow us to uniquely define the characteristics of a star for any model of the EOS. At present, it is impossible to uniquely select a specific model for the EOS. As a criterion for this selection should be the comparison of the results of theoretical calculations of the integral parameters of superdense stars with observational data on pulsars. Unfortunately, the state of the art calculations do not have sufficient accuracy. Until recently, the mass $M = 1.442 \pm 0.003 M_\odot$ of the double pulsar PSR $1913 - 16$ was considered the most well-determined mass measurement [1]. In recent years new accurate measurements were reported of the masses of two pulsars each of which is in binary orbit with a white dwarf. Their reported masses are very close to two solar masses: for PSR $J1614 - 2230$ $M = 1.97 \pm 0.04 M_\odot$ [2] and for PSR $J0348 + 0432$ $M = 2.01 \pm 0.04 M_\odot$ [3]. These discoveries put certain constraints on the EOS of baryonic superdense matter.

In the first part of the presented work (Section 2) we determine sets of values of the MIT bag model constants. These are then used in the EOS of strange quark matter (SQM). We show that they yield a maximal mass M_{max} of the equilibrium quark configurations which exceeds the recently accurately determined mass $2.01 M_\odot$ of the radio pulsar PSR $J0348 + 0432$ in a binary. We show that if the quark-gluon interaction constant α_c is limited to values $\alpha_c < 0.6$, then all of the three pulsars with the most accurately measured masses ($M/M_\odot = 1.44, 1.97$ and 2.01) may be candidates for strange stars.

If quark matter is not self-bound, then there may exist the so-called hybrid stars. The maximum mass of such stars is determined by the EOS of ordinary nuclear and nucleonic matter (where quarks are confined into hadrons) and by the EOS of deconfined quark matter. The question we address is the following: what are the possible combinations of these EOS that can provide a maximum mass for hybrid stars greater than $2.01 M_\odot$? The second part of this contribution (Section 3) is dedicated to this issue.

If, indeed, SQM exists as a form of self-bound matter, then there may be celestial bodies which are called strange dwarfs (SD) [4, 5, 6]. These stars are composed of quark matter core with a mass $M_{\rm core} \lesssim 0.02 M_\odot$ and an extended outer crust which consists of degenerate electrons and nuclei [the so-called (Ae) matter]. The mass-radius relation for these stars is determined in the third part of this paper (Section 4) for different chemical compositions of the outer shell is defined. Here we also identify the probable strange dwarf candidates among the observable white dwarfs.

2. The Pulsar PSR J0348+0432 and Strange Stars

The energy density ρ of superdense stars is usually expressed in terms of the average energy ε per baryon and the baryon concentration n (the number of baryons per unit volume) by the formula $\rho = (m_0 c^2 + \varepsilon(n))n$, where m_0 is either set equal to the neutron mass m_n or, as we will do in this paper, to the mass per nucleon in the iron nucleus $M(^{56}{\rm Fe})/56$. As well known from the extensive studies of physics of superdense stars, neutron stars configurations with masses close to their maximum mass $M_{\rm max}$ have central densities ρ_c which are by an order of magnitude larger than the nuclear saturation density. This is true for superdense stars composed of nucleons (with a

possible admixture of hyperons) that do not contain quarks; these objects we shall nominally refer to as neutron stars. For rigorous EOS of baryon matter, see for example [7, 8], the neutron star masses are of the order of one solar mass for central densities comparable to nuclear saturation density. On the other hand, because quark matter within the MIT bag model [9] is characterized by extremely low compressibility, the transition to the SQM phase takes place at baryon concentrations $n_{\min} < 2n_0$, where $n_0 = 0.15\text{fm}^{-3}$ is the nuclear concentration (see Table 1). These densities are considerably below the central density ρ_c of the neutron star with maximal mass $M_{\max}$. Therefore the transition to SQM matter takes place before neutron stars lose their stability. This has the consequence that within the bag model neutron star and compact stars with SQM will form a single family of stars on the $M(\rho_c)$ diagram [10, 11]. On the other hand the softness of SQM EOS would imply $M_{\max} < 2.01 M_\odot$ for such configuration in contradiction with observations.

In this contribution we assume a bag model for quark matter [9] that depends on three phenomenological constants: the bag constant B (vacuum pressure), the quark-gluon interaction constant α_c, and the strange quark mass m_s. We determined [12, 13] those sets of values of these constants which predict such an EOS of SQM that yields a maximum mass of the equilibrium configurations which exceeds the mass PSR $J0348 + 0432$, $M_{max} > 2.01 M_\odot$.

2.1 The Transition to SQM

It has been shown in Refs. [14, 15, 16] that SQM consisting of u, d and s quarks can be energetically more favorable, even at zero pressure, than nonSQM (NQM) consisting of u and d quarks and the matter in atomic nuclei (N). Ref. [17] showed that within the bag model [9] description of the SQM that it consists of roughly equal amounts of u, d and s quarks with a small admixture of electrons which ensures electrical neutrality. Furthermore, it was shown that for certain values of the bag constants (B, α_c, m_s), the average energy ε per baryon as a function of the specific baryon volume $(1/n)$ can have not only a positive but also a negative local minimum, which in its turn leads to two alternatives EOS, which we address in turn.

The first case corresponds to $\varepsilon_{\min} > 0$. For quark densities greater than $n_{\min}$ a first order phase transition takes place between nuclear and SQM with a jump in density. Here, in accord with the Gibbs condition (or by a Maxwell construction) a phase equilibrium is established between the SQM and nucleon-hyperon (nuclear) matter. Thus, these two phases may coexist simultaneously. Superdense stars based on the EOS of this type are referred to as hybrid stars. These stars with $M \geq M_\odot$ have a central core consisting of *SQM* and low-density shell which consists of ordinary neutron star matter. More that 90% of the mass of such configuration is concentrated in the SQM core. These configurations are discussed in the next section of this review.

The second alternative corresponds to the case $\varepsilon(n_{min}) < 0$, which is of special interest. In this case a Maxwell construction is not possible; i.e., a phase transition from nuclear to SQM is not possible. However, quark matter can be self-bound, so that instead of object bound by gravity self-confining objects known as "strange stars" (SS) can arises [18, 19]. These stars can also exist in the absence of gravitation. The maximum mass of these configurations, as in the case of neutron stars, should be of the order $2M_\odot$. Models of strange stars have been discussed and analyzed comprehensively in Refs. [20, 21]. Research on SQM and its relation to superdense stars has been reviewed in Ref. [22].

2.2 Computational Results

The main parameters of spherically symmetric static superdense stars are determined by numerical integration of a system of relativistic equations for stellar equilibrium, the Tolman-Oppenheimer-Volkoff (TOV) equations [23, 24]. For any given value for star's central energy density ρ_c TOV equations determine the star's radius R (defined by $P(R) = 0$, where P is the pressure), gravitational mass

$$M = (4\pi/c^2) \int_0^R \rho r^2 dr, \tag{2.1}$$

where ρ is the energy density, rest mass

$$M_0 = (4\pi m_0) \int_0^R n r^2 \exp(\lambda/2) dr, \tag{2.2}$$

where n is the baryon number density, and $\exp(\lambda)$ is the radial component of the metric tensor, proper mass

$$M_p = (4\pi/c^2) \int_0^R \rho r^2 \exp(\lambda/2) dr, \tag{2.3}$$

and the redshift Z_s

$$Z_s = (1 - 2GM/c^2 R)^{-1/2} - 1 \tag{2.4}$$

on the star's surface.

For any given triplet of bag parameters, we first determine the $\varepsilon(n)$ dependence and the values of n_{min}, $\varepsilon_{\min} = \varepsilon(n_{\min})$ for which the pressure $P = 0$. If $\varepsilon_{min} < 0$ the surface defined by $P = 0$ corresponds to that of SS and if $\varepsilon_{min} > 0$ then it corresponds to a surface of the quark core of a hybrid star. For each EOS the dependence of the mass of the equilibrium stable configurations as a function of the central energy density ρ_c, i.e., the $M(\rho_c)$ curve, is found by integrating the TOV equations. The maximum masses M_{max} at which stability is lost [25, 26] are found for each series. Calculations were done for $\alpha_c = 0.05, 0.5$, and 0.6 and strange quark masses $m_s c^2 = 150 \div 200$ MeV, which are on the order of the difference in the masses of the Λ^0 hyperon and a nucleon. Note, that these values for strange quark mass exceed the current quark mass value for this flavor, which is approximately equal to 95 MeV [27]. It is conditioned by the fact that quarks are not asymptotically free at the density region considered in this work.

We list in Table 1 the integral parameters of stellar configurations with maximum mass for some example EOS defined by the values of m_s, B, and α_c. Table 1 and Fig. 1 demonstrate that out of the three parameters of the bag model, i.e. B, α_c, m_s, the bag constant B is decisive in determining the maximum mass of a stellar configuration. We see that as B increases, $M_{\max}$ decreases and, at a critical value B_0, yields a mass less than $2.01 M_\odot$. Only those equations of state for which $B \leq B_0$ are compatible with observations.

We note that, even though the maximum mass of configurations can be increased by decreasing the value of the bag constant B, which makes the EOS compatible with observations, the transition to SQM occurs at unrealistically low densities, which are slightly above the nuclear density. For example, if we assume $B = 30$ MeV/fm^3, $m_s = 150$ MeV and $\alpha_c = 0.05$) we have $M_{max}/M_\odot =$

Table 1: Integral Parameters of Maximum Mass Configurations, corresponding to the EOS with $\alpha_c = 0.5$ and $\alpha_c = 0.6$.

m_s MeV	B MeV/fm^3	$\varepsilon_{\min}$ MeV	$n_{\min}/n_0$	$\frac{M_{\max}}{M_\odot}$	$\frac{M_0}{M_\odot}$	$\frac{M_p}{M_\odot}$	ρ_c 10^{15}g/cm^3	R km
$\alpha_c = 0.5$								
150	35	-81.5	1.24	2.336	3.062	2.959	1.42	12.95
150	40	-55.9	1.37	2.198	2.798	2.787	1.62	12.16
150	45	-32.5	1.49	2.084	2.584	2.641	1.79	11.52
150	48	-19.5	1.56	2.023	2.473	2.567	1.92	11.17
150	51	-6.95	1.63	1.968	2.374	2.496	2.02	10.86
200	35	-60.3	1.25	2.235	2.847	2.823	1.52	12.54
200	40	-34.9	1.37	2.105	2.607	2.661	1.73	11.78
200	44	-16.3	1.48	2.017	2.449	2.549	1.86	11.28
200	45	-11.8	1.51	1.997	2.413	2.524	1.90	11.17
200	47	-3.09	1.55	1.959	2.345	2.477	2.00	10.93
$\alpha_c = 0.6$								
150	35	-64.1	1.22	2.337	3.002	2.961	1.41	12.94
150	40	-38.1	1.34	2.200	2.745	2.790	1.61	12.15
150	45	-14.3	1.46	2.086	2.536	2.647	1.81	11.5
150	50	7.58	1.58	1.989	2.362	2.523	1.98	10.96
150	52	15.9	1.63	1.953	2.300	2.478	2.05	10.77
200	35	-43.8	1.23	2.231	2.789	2.817	1.52	12.51
200	40	-18.1	1.36	2.103	2.558	2.658	1.72	11.76
200	44	0.74	1.46	2.016	2.404	2.551	1.89	11.25
200	45	5.25	1.49	1.996	2.369	2.526	1.92	11.14
200	47	14.1	1.54	1.959	2.303	2.478	1.99	10.92

2.52, but the transition density is only $n_{\min}/n_0 = 1.16$, where n_0 is the nuclear concentration of baryons. Such low transition densities render the underlying EOS unrealistic. The same trend can be observed from Table 1, which implies that even for the bag model EOS producing liming values of maximal mass $M_{\max}/M_\odot \approx 2.01$, the transition to strange quark matter takes place at densities below twice the nuclear density, $n_{min}/n_0 \leq 1.7$.

The configurations containing SQM that have been examined in terms of the bag EOS are characterized by extremely low compressibility. Thus, as opposed to neutron stars, the radii of these configurations increase with increasing mass. Only prior to the onset of instability close to the maximal mass this scaling stops because of general relativistic effects.

By definition the rest mass M_0 is equal to the total baryon number N_B of the equilibrium configurations consisting of SQM multiplied by m_0, i.e., $M_0 = m_0 N_B$. Thus, the difference $(M - M_0)$ determines the binding energy E_B of these configurations and the packing coefficient $f = 1 - M/M_0$. While this quantity is less than 1% for ordinary atomic nuclei, for neutron star configurations with M_{max} it can reach 12% [28]. For configurations consisting of SQM, which are SS with $\varepsilon_{min} < 0$ in the overwhelming majority of cases, it is considerably higher. Thus, for the configurations with

M_{max} and $\alpha_c = 0.05$, $B = 40$ then $f = 0.26$, while for those with M_{max} and $\alpha_c = 0.6$, $B = 40$ then $f = 0.26$.
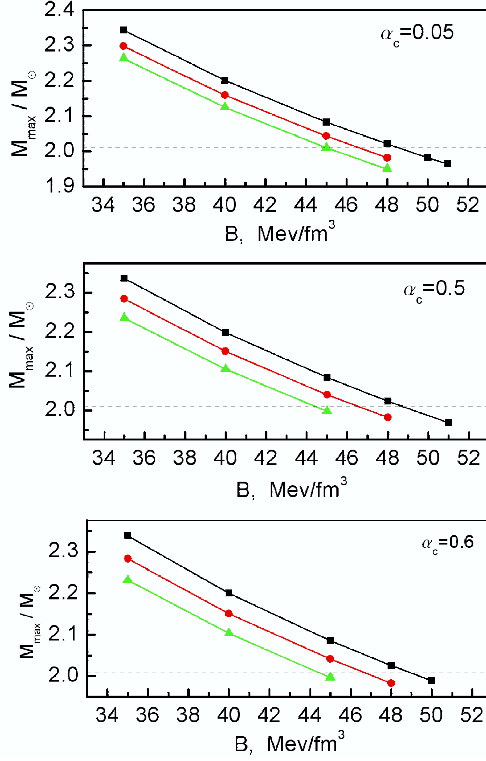
Figure 1: The maximum mass of equilibrium configurations as a function of the parameter B for different values of the strange quark mass m_s: ■ − $m_s = 150$ MeV, ● − $m_s = 175$ MeV, and ▲ − $m_s = 200$ MeV and three values of the parameter α_c indicated in the panels. The dashed line corresponds to the configuration with $M/M_\odot = 2.01$.
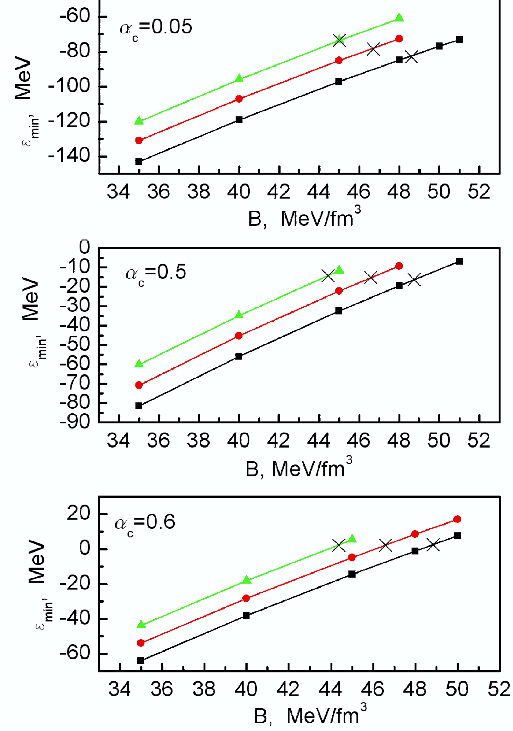
Figure 2: The minimum average energy per baryon ε_{min} as a function of B for EOS leading to $M_{max}/M_\odot \geq 2.01$ for different values of the strange quark mass m_s and α_c. The crosses indicate the maximum possible values of ε_{min}. The notation is as in Fig. 1.

Figure 1 shows the dependence of M_{max} on B for three values of α_c and three values of the strange quark mass m_s. The dashed line corresponds to the limiting configuration with mass $M_{\text{max}}/M_\odot = 2.01$ and determines the value of B_0 for the different values of m_s. Recall that only those EOS for which $B \leq B_0$ are compatible with astronomical observations.

Figure 2 shows analogous plots as in Fig. 1, but for ε_{min} as a function of B. The crosses on the lines mark the values of ε_{min} corresponding to B_0. We denote these values by $(\varepsilon_{min})_0$. Only those equations of state for which $\varepsilon_{min} < (\varepsilon_{min})_0$ are compatible with astronomical observations. We can see from Table 1 and Figs. 1 and 2 that B_0 depends very weakly on α_c: it decreases slightly with increasing strange quark mass, but remains within the narrow interval of values $44 < B_0 < 49$.

Our calculations show that when $\alpha_c \leq 0.5$ we have $(\varepsilon_{min})_0 < 0$. Therefore all the EOS which satisfy this condition describe SS stars; the integral parameters for such stars are listed in Table 1 (see also Figure 2).

Table 1 lists also data for the case $\alpha_c = 0.6$. Here the distinction between SS and hybrid star configurations depends on the values of other parameters as well and one may have both $\varepsilon_{min} < 0$ (SS configurations) and $\varepsilon_{min} > 0$ (hybrid star configurations). However, in the limiting case where B approaches to B_0 (M_{max} decreases and approaches to $2.01 M_\odot$), we have $(\varepsilon_{min})_0 > 0$, i.e., we find configurations consisting of SQM that correspond to hybrid stars. However, as Figure 2 implies, even in the case of $\alpha_c = 0.6$, the overwhelming majority of the EOS have $\varepsilon_{min} < 0$; i.e., in this case, as well, most of the EOS yield strange stars.

In the range of parameter values $0.6 < \alpha_c < 1$ we find EOS which predict configurations of hybrid stars with SQM cores and masses $M_{max}/M_\odot > 2.01$. However, some caution is needed here since we have used the results of Ref. [17], which determines the basic thermodynamic quantities of SQM via perturbation theory with respect to the small quark-gluon interaction. More precisely, these computations where carried out to first order with respect to the small expansion parameter $(2\alpha_c/\pi)$; clearly the perturbative expansion fails for the values of α_c mentioned above.

2.3 Summary to Sec. 2

In this section we have studied possible limitations on the EOS of superdense baryon matter imposed by precise measurements of the masses of two radio pulsars with $M \sim 2M_\odot$ during last few years [2, 3]. Our study of the EOS of SQM matter within the bag model [9] shows that the transition to SQM takes place at densities less than twice the density in atomic nuclei. This density is well below the central energy density of most massive neutron stars. Thus in the framework of the bag model we find that the low-mass neutron stars and superdense stars consisting of SQM form a single family of compact stars, i.e., are described by a single $M(\rho_c)$ curve in the mass vs central density diagram. We have found sets of values of the phenomenological constants for the bag model (B, α_c, m_s) which yield maximal masses of the equilibrium configurations in excess of the measured mass of PSR $J0348 + 0432$ ($M_{max} > 2.01 M_\odot$) using EOS of SQM. Our study shows that for the values of the quark-gluon interaction constant $\alpha_c < 0.6$, the resulting EOS predict SQM in stellar models with masses corresponding to those most accurately measured for known pulsars, specifically $M_{max}/M_\odot = 1.44, 1.97, 2.01$. Thus, we conclude that these objects would be strange stars.

3. Maximum masses of hybrid stars

In this section we consider sets of the values of the MIT bag model parameters for which the condition $\varepsilon_{min} > 0$ is fulfilled. As already discussed in Sec. 2, this is a necessary condition for the phase coexistence of quark gluon plasma and hadron matter. The hadron matter close and above the nuclear saturation density will be described by an EOSs which were obtained in the framework of the relativistic nuclear field theory [29]. Specifically we will use the model constructed on a basis of a potential [30, 31, 32], where the impact of the two-particle correlations is taken into account in the so-called λ^{00} - approximation [33, 34]. These EOSs, which are marked as "Bonn" and "HEA", were merged with the EOS of Baym-Bethe-Pethick (BBP) which is valid in the density range below half the nuclear saturation density and above the neutron drip density [35]. As an example of an EOS that is more stiff than the EOSs "Bonn" and "HEA" we use in our calculations the EOS of Bethe-Johnson (BJ-V) [36].

7
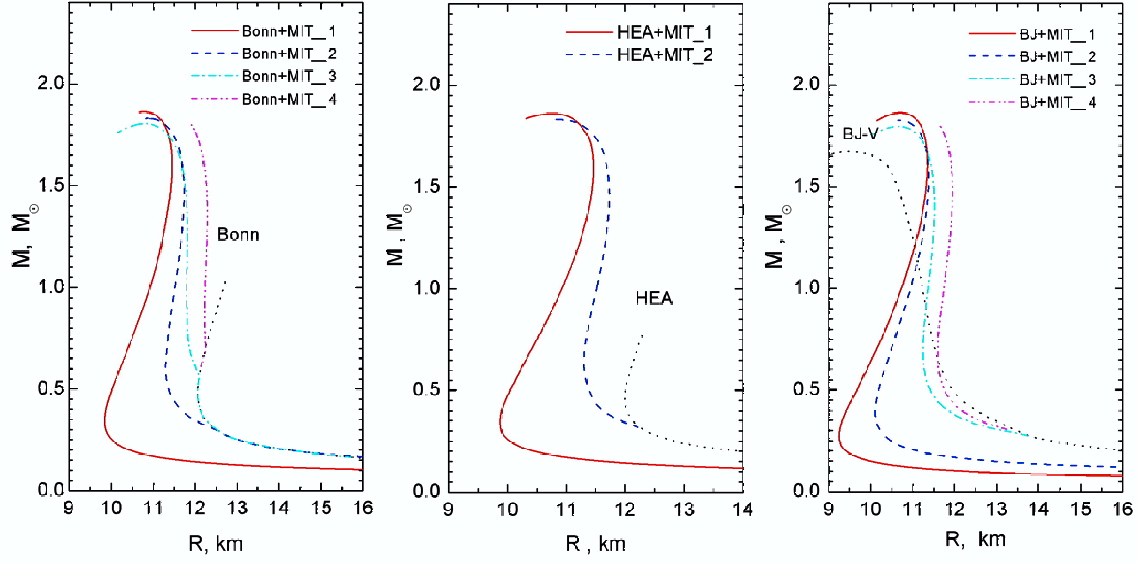
Figure 3: The mass-radius relations for hybrid stars constructed from various combinations of the three EOSs of hadronic matter and four EOSs of quark matter based on MIT bag model.

Following Refs. [37, 38], we assume that the surface tension between the hadronic and the SQM phases is high enough so that the phase transition is the ordinary first-order phase transition, i.e., the pressure during the phase transformation remains constant, and the density undergoes a jump. In this case, the transition parameters are defined through the Maxwell construction. By combining the above three EOSs of hadronic matter "HEA", "Bonn" and "BJ-V" with four EOSs for quark-electron u, d, s, e plasma, calculated in the framework of the MIT bag model in accordance with the values of the model parameters given in Table 2, we obtain ten distinct EOSs. The phase transition in all these EOSs is of Maxwell-type. We then integrated the TOV equations for this set of EOS to find the integral parameters of hybrid stars.

Table 2: MIT bag model parameters for different variants of SQM EOS with $\varepsilon_{min} > 0$.

Quark Model	m_s MeV	B MeV/fm^3	α_c	ε_{min} MeV	n_{min} fm^{-3}
MIT-1	175	55	0.5	10.44	0.258
MIT-2	200	55	0.5	20.71	0.263
MIT-3	175	55	0.6	28.61	0.258
MIT-4	175	60	0.5	28.97	0.276

Figure 3 shows the mass-radius relationship for hybrid stars, where each panel corresponds to a different EOS of the hadron component.

Table 2 lists the MIT bag model parameters of the EOSs of quark matter component used in our calculations. We also give the values of energy per baryon ε_{min} and baryon number density n_{min} corresponding to the minimum energy state. Table 3 presents the values of parameters of hybrid star configurations with maximum gravitational mass for various combinations of the EOS

of hadronic and quark matter phases.

Table 3: Parameters of hybrid star configurations with maximum gravitational mass.

Hadronic EOS	Quark EOS	ρ_c 10^{15}g/cm^3	$\frac{M_{\max}}{M_\odot}$	R km	$\frac{M_0}{M_\odot}$	R_{core} km
HEA	MIT-1	2.1.05	1.863	10.65	1.845	10.33
	MIT-2	2.2.80	1.831	10.88	1.707	9.77
Bonn	MIT-1	2.241	1.864	10.77	1.847	10.26
	MIT-2	2.283	1.831	10.87	1.713	9.79
	MIT-3	1.407	1.820	10.85	1.438	9.61
	MIT-4	2.359	1.806	10.81	1.594	9.28
BJ-V	MIT-1	2.214	1.863	10.72	1.790	10.32
	MIT-2	2.302	1.826	10.67	1.809	10.11
	MIT-3	1.407	1.799	11.65	1.629	10.22
	MIT-4	2.413	1.796	10.64	1.695	9.59

The results of our calculations, presented in Table 3, show that within the framework of the MIT bag model, the maximum masses of the hybrid star do not reach the value $2.01M_\odot$. Note that, for sufficiently small values of the bag constant B which result in a positive value of the energy per baryon, the value of the hybrid star masses can reach the required value $2.01M_\odot$. However, in such configurations the phase transition from hadronic to quark matter occurs at a densities below the normal nuclear density. Therefore, such low values of the B parameter should be considered as unrealistic.

Despite the fact that models for EOS considered in this section do not allow us to obtain values of masses of hybrid stars $M > 2.01M_\odot$, this is not yet a proof of absence of deconfined quarks inside stellar cores. Investigations of hadronic phases and their EOS in the framework of relativistic mean field theories shows that the inclusion of scalar-isovector interaction channel leads to a more stiff EOS and, consequently, to an increase in the maximum masses of neutron stars [39]. Alternative models of quark matter phase, such as, for example, the NJL model [40], also predict stiffer EOS for quark matter than the MIT bag model considered here. We relegate the investigation of the EOS of superdense matter with a first order phase transition on the basis of these models to future work. This will allow us to carry out a complete analysis of characteristics of hybrid stars and in particular to clarify the issue of maximum possible mass of such objects.

4. Mass-radius relation of the strange dwarfs: theory vs observations

If the SQM is self-bound, then there may exist celestial bodies which consist of a quark core with mass $M_{\mathrm{core}} \leq 0.02M_\odot$ and an external shell consisting of lattice of nuclei with a charge neutralizing background of degenerated electrons (the so-called Ae matter). These objects are called strange dwarfs (SD) [4, 5, 6].

The strong electrostatic field on the surface of the quark core ($\sim 10^{18}$V/cm) prevents the penetration of Ae matter into the quark core [20]. The maximum density of the matter in ordinary white

dwarfs (WD) is limited to a value in the range $10^9 - 10^{10}$g/cm^3. In SD the maximum density of matter of the envelope residing over the quark core is given by the density of the drip of neutrons from nuclei which is in the range $\rho_{drip} = (2-5) \cdot 10^{11}$g/cm^3 The stability of SD was studied in Ref. [5, 41, 42].

The radii of WD and SD which have same masses differ insignificantly. In the case of SD the larger is the portion of the mass of the quark core, the smaller is the radius of the strange star. Depending on M_{core} this difference can reach up to 10% for stars with masses $M \sim 0.3 - 1M_\odot$. The WD and SD is difficult to distinguish by their radii, because of the small difference in this parameter. Therefore, it is not an easy task to search for SD candidates among the known WD-type objects. Observationally, the masses and radii of the white dwarfs should be "measured" with sufficient accuracy. At the same time, theoretical calculations needed to take into account all the decisive factors. For non-rotating WD and SD these factors are the chemical composition and the equation of state of *Ae* matter.

In Ref. [43] it was assumed that the *Ae* matter in WD and SD is in the state of minimum energy, in which case the *Ae* plasma consist of nuclei of iron group. In such matter the chemical composition, the energy density and the pressure are uniquely determined by the concentration of baryons. The *Ae* matter in SD and WD can reach such state only after a very long evolution. The time-scale of this transition assuming a "quiet" evolution is more than the cosmological time-scale. Even in case of supernova explosion the nuclear transformations do not lead the matter to the state of minimum energy. Therefore, the final chemical composition during such an explosive evolution would be also different from the state of minimum of energy [44]. Therefore the existence of WD which consist of only (or mostly) iron nuclei is questionable. Thus, the assumption of Ref. [43] that matter in WD and SD can be described by EOS based on state of minimum energy may not apply. It is known, that the closer the matter is to the state of minimum energy, the smaller is the radius of the star. Therefore, the radii obtained in Ref. [43] for these stars correspond to an extreme compact limit of such stars and, therefore, place a lower limit on R.

4.1 Characteristics of *Ae* and quark matter phases

We start with a summary of the EOS of a cold degenerate matter used to determine the parameters of WD and SD. We use the EOS of Ref. [45] for densities below the density $\rho_1 = 11.4AZ$ (g/cm^3), where A is the mass number and Z is the atomic number (charge) of nuclei. At density ρ_1 the average distance between atoms is equal to the size of the atom. For $\rho > \rho_1$ we use the EOS derived in Ref. [46]. This EOS accounts for the Coulomb interactions of electrons, the correlation and exchange effects, as well as inhomogeneous distribution of electrons in the vicinity of the nuclei. Within the range of densities $\rho_1 \leq \rho \leq \rho_2 = 8.33AZ^2$(g/cm^3) the plasma becomes full ionized by the pressure. Here ρ_2 is the density at which the average distance between the electrons is equal to the radius of the K-shell of the atom. The effect of pressure ionization is also taken into account in Ref. [46].

Below we describe our effort to find candidates for the SD in the list of known WD. For this we determine theoretically the areas of mass-radius $(M - R)$ plane where the SD are located. We confront these results with the known information on WD object by showing these objects in the same diagram. The location of WD on this plane depends on the chemical composition of the stellar matter. In the case of SD, their area of location in the $(M - R)$ plane also depends on the

mass and radius of the quark core. Following Ref. [47] we computed the integral parameters of WD and SD which consist of nuclei with mass numbers $A = 12$, 16, 24, and 56. It is assumed that the mass number A of the nuclei in the star does not depend on the density and the atomic number Z is determined from the $\beta-$ equilibrium condition. We used the experimental data for the masses of these nuclei [48] to determine the thresholds of neutronization of individual nuclei and the density when a free neutron gas is formed in the *Ae* matter. For isobars of iron group ($A = 56$) the experimental data for $Z < 20$ is not available. Therefore for this group Weizsacker's formula was partially used.

As noted above, a strong electrostatic field on the surface of the quark core prevents the penetration of atomic nuclei into the core. In the presence of degenerated Ae matter above the quark core the strength of this field and the charged layer thickness decrease. The greater the density of *Ae* matter is, the weaker is the electric field and thinner the charged layer. When the Fermi energy of the electrons in *Ae* matter and the Fermi energy of the electrons in the quark matter are equal then the electric field disappears completely [20]. If the equality of these Fermi energies is achieved at some density $\rho_0 < \rho_{\text{drip}}$ then the maximum density of *Ae* matter ρ_{max} at the base of the *Ae* envelope is ρ_0, otherwise $\rho_{\text{max}} = \rho_{\text{drip}}$.

The parameters of the quark core are determined on the basis of the EOS of SQM according to the MIT bag model. We use the accepted values of the parameters of this models in our numerical calculations: the bag constant $B = 60$ MeV/fm^3, the strange quark mass $m_s = 175$ MeV and the constant of the quark-gluon interactions $\alpha_c = 0.05$.

4.2 Numerical calculations and comparison with the observational data

We have determined the integral parameters of WD and SD by integrating the TOV equation [23, 24]. Our results for the radius-mass relations (i.e. the curves $R = R(M)$) for the WD are presented in Fig. 4 by solid lines - black for carbon WD, red for magnesium WD and blue for iron WD. These curves replicated the results of [47]. Unlike the WD, the strange dwarfs fill in the individual stripes labeled in the figure as *CSD* for carbon, *MgSD* for magnesium and *FeSD* for iron envelopes. Each $R = R(M)$ curve of WD is the upper boundary of the corresponding stripe of SD. The curve $R = R(M)$ of SD with $\rho_{tr} = \rho_{drip}$ (dashed curve of the corresponding color) is the lower limit of this stripe. The position of SD with a given mass in the stripe depends on the proportion of the mass of the quark core M_{core}. The larger M_{core} is, the lower is the location of the SD in the stripe. Those stripes of iron, magnesium and carbon SD are shown on Fig. 4. The results of the calculations for oxygen WD and SD are not shown in Fig. 4, as the stripe of these stars overlap with those of carbon and magnesium SD.

The assumption that the *Ae* matter in the WD and SD contains only one type of isobars is an idealization. Furthermore, the stripes of carbon, oxygen and magnesium SD overlap, therefore we can consider a combined region covered by these stripes where SD may reside. WD and SD with the mixed chemical composition (carbon-oxygen-magnesium) will be located in a one common stripe in the $R - M$ plane. One can distinguish by mass and by radius such WD from SD. If the matter of stars contains only the nuclei with mass numbers in the range $24 \leq A \leq 56$, then on the plane $M - R$ the WD will be located between magnesium and iron WD, and the SD will be located below the magnesium WD including the iron stripe. The greater the relative content of iron in such star is, the closer to the iron SD is its position on the $M - R$ plane. However, the presence of a big

11
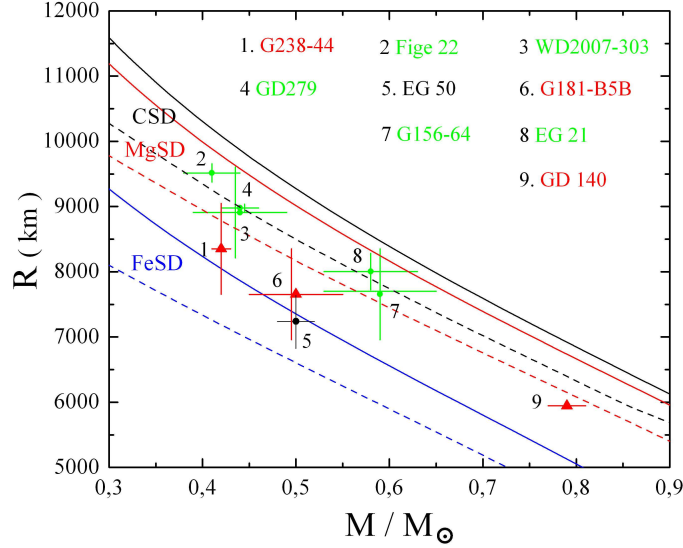
Figure 4: The mass-radius $M - R$ relations of the carbon, magnesium and iron white dwarfs (the black, red and blue solid lines accordingly). The curves $R = M(R)$ of the carbon, magnesium and iron strange dwarfs with $\rho_{tr} = \rho_{drip}$ (dashed curve of the corresponding color). Between the solid and dashed curves are the corresponding stripes of the carbon, magnesium and iron (*CSD*, *MgSD* and *FeSD*) strange dwarfs. It is marked the locations of known white dwarfs with errors in the determination the masses and radii.

amount of nuclei with $A > 24$ in SD is improbable. Therefore, the wide area between the $M(R)$ curve (solid blue line in Fig. 4) of the iron WD and the stripe of magnesium SD should be almost empty. Thus, the stars that are between the regions *MgSD* and *FeSD* in Fig. 4 are either WD or SD the matter of which contains nuclei $A > 24$. Below the curve $R = R(M)$ of the iron WD (region *FeSD*) only iron strange dwarfs can exist. The closer a star is to *FeSD*, the higher is the probability that this star is a SD.

4.3 Comparison with the observational data and critical remarks

The masses and radii of WD which are relatively accurately defined by the observational data are given in Refs. [49, 50]. The positions of nine white dwarfs on the $M - R$ plane are shown in Fig. 4. We have selected those stars whose parameters are defined with low errors and are in the region of possible SD. The Fig. 4 also shows the errors in determining of masses and radii.

As in Ref. [43] we assume that the WD $EG - 50$ (black circle) with a very high probability is a SD. The stars $G238 - 44$ and $G181 - 135B$ (red triangles) are close to the region of *FeSD*, but their parameters are determined not precisely enough. Therefore, we can only indicate that they are possible candidates to be SD.

The mass and radius of the star $GD - 140$ are defined with very small errors. If the matter of this star contains a small number of nuclei of $A > 24$ then it is also most likely a SD. The rest of the selected stars (green circles) are in region of the $M - R$ plane, where the existence of SD is theoretically possible. However, it is unlikely that among these stars there are SD.

The masses and radii of the observed WD are determined indirectly, i.e., by processing the observational information on other parameters. This is done on the basis of certain theoretical

models of WD. Therefore, we need to be aware of the fact that the extraction of information on the mass and radius may contain theoretical background which is not compatible with our models of SD. Part of the uncertainties are related to the measurements of WD/SD luminosities which actually give an information on the radius of the radiating region, which need not be the radius of the star. It is known that those two radii are slightly different. However, are the numerical values of these radii close enough in order to distinguish a WD from a SD? An analysis of uncertainties involved in the mass/radius determination for WD is needed to answer this and related questions.

In closing this section we note that we considered so far only non-rotating configurations. A rotating configuration experiences centrifugal stretching and may have a radius larger than its non-rotating counterpart (in the plane orthogonal to the rotation axis). This implies that the region of $M - R$ plane which can be populated by WD and SD may expand if we allow for the rotation of these objects. Consequently, there could be, for example, pure iron hot strange dwarfs above the region where the cold iron strange dwarfs (region *FeSD*) reside. These issues require a separate study.

4.4 Summary to Sec. 4

Here we provide a brief summary of the key results of this section:

- The regions of the existence of WD and SD overlap on the mass-radius plane. There might exist SD among the observed WD which could have the same masses and radii as the WD counterpart.

- The observed WD which are located below the curve $R = R(M)$ for iron white dwarfs are suggested to be SD.

- We need to find other distinguishing characteristics for non-iron SD that can discriminate them from non-iron WD, because both types of objects have similar in masses and radii.

- The WD $EG - 50$ is with high probability a SD, whereas $G238 - 44$, $G181 - 85B$ and $GD - 140$ are good candidates for being a SD.

References

[1] J.H. Taylor, J.M. Weisberg, *Astrophys. J.* **345** (1989) 434 .

[2] P. Demorest et al., *Nature* **467** (2010) 1081.

[3] J. Antoniadis et al., *Science* **340** (2013) 1233232.

[4] N.K. Glendenning, Compact Stars: *Nuclear Physics, Particle Physics, and General Relativity*, Springer, Heidelberg 2000.

[5] N.K. Glendenning, Ch. Kettner, F. Weber, *Astrophys. J.* **450** (1995) 253.

[6] Yu.L. Vartanyan, A.K. Grigoryan, T.R. Sargsyan, *Astrophysics* **47** (2004) 223.

[7] B.D. Serot, *Phys.Lett.* **B86** (1979) 146.

[8] V.R. Pandharipande, D. Pines, and R.A. Smith, *Astrophys. J.* **208** (1976) 550.

[9] A. Chodos, R.L. Jaffe, K. Johnson, C.B. Thorn, V.F. Weisskopf, *Phys. Rev.* **D9** (1974) 3471.

[10] Yu.L. Vartanyan, A.R. Arutyunyan, A.K. Grigoryan *Astrophysics* **37** (1994) 271.

[11] Yu.L. Vartanyan, A.R. Arutyunyan, A.K. Grigoryan, *Astron.Lett* **21** (1995) 122.

[12] Yu. L. Vartanyan, A. K. Grigoryan, A.A. Shahinyan, *Astrophysics* **58** (2015) 276.

[13] Yu. L. Vartanyan, A. K. Grigoryan, A.A. Shaginyan, *Astronomy Letters*, **41** (2015) 343.

[14] A.R. Bodmer, *Phys. Rev.* **D4** (1971) 1601.

[15] H. Terazawa, JNS-Report-336 JNS, *University of Tokyo*,(1979)

[16] E. Witten, *Phys. Rev.*, **D30** (1984) 272.

[17] E. Farhi, R.L. Jaffe, *Phys. Rev.*, **D30** (1984) 2379.

[18] C. Alcock, A. Olinto, *Ann. Rev. Nucl. Part. Sci.* **38** (1988) 161.

[19] O.G. Benvenuto, J.E. Horvarth, *Phys. Rev. Lett* **63** (1989) 716.

[20] C. Alcock, E. Farhi, A. Olinto, *Astrophys. J.* **310** (1986) 261.

[21] P. Hansel, J.L. Zdunik, R. Shaeffee, *Astron. Astrophys* **160** (1986) 12.

[22] F. Weber, *Prog. Part. Nucl. Phys.* **54** (2005) 193.

[23] R.C. Tolman, *Phys. Rev.*, **55** (1939) 364.

[24] J.R. Oppenheimer, G.M. Volkoff, *Phys. Rev.* **55** (1939) 374.

[25] Ya.B. Zel'dovich, *Voprosy kosmogonii (Problems of Cosmogony)* **9** (1963) 36. [in Russian]

[26] G.S. Bisnovatyi-Kogan, *Astron. Astrophys.* **31** (1974) 3910.

[27] K.A. Olive et al. (Particle Data Group), *Chin. Phys.* **C 38** (2014) 090001.

[28] G.S. Sahakyan, Yu.L. Vardanyan, *Sov. Astron.* **8** (1964) 147.

[29] F. Weber, N.K. Glendenning, M.K. Weigel, *Astrophys. J.* **373** (1991) 579.

[30] R. Machleidt, K. Holinde, Ch. Elster, *Phys. Rep.* **149** (1987) 1.

[31] K. Holinde, K. Erkelenz, R. Alzetta, *Nucl. Phys.* **A194** (1972) 161.

[32] K. Holinde, K. Erkelenz, R. Alzetta, *Nucl. Phys.* **A198** (1972) 598.

[33] P. Poschenrieder, M.K. Weigel, *Phys. Lett.* **B200** (1988) 231.

[34] P. Poschenrieder, M.K. Weigel, *Phys. Rev.* **C38** (1988) 471.

[35] G. Baym, H.A. Bethe, C. Pethick, *Nucl. Phys.* **A175** (1971) 225.

[36] R.C. Malone, M.B. Johnson, H.A. Bethe, *Astrophys. J.* **199** (1975) 741.

[37] G.B. Alaverdyan, A.R. Harutyunyan, Yu.L. Vartanyan, *Astrophysics*, **46** (2003) 361.

[38] G.B. Alaverdyan, A.R. Harutyunyan, Yu.L. Vartanyan, *Astrophysics*, **47** (2004) 52.

[39] G.B. Alaverdyan, *Research in Astron. Astrophys.* **10** (2010) 1255.

[40] Y. Nambu and G. Jona-Lasinio, *Phys. Rev.* 122 (1961) 345.

[41] Yu.L. Vardanyan, G.S. Hajyan, A.K. Grigoryan, T.R. Sarkisyan, *Gravitation and Cosmology* **15** (2008) 188.

[42] Yu.L. Vardanyan, G.S. Hajyan, A.K. Grigoryan, T.R. Sarkisyan, *Astrophysics* **55** (2012) 98.

[43] Yu.L. Vartanyan, G.S. Hajyan, A.K. Grigoryan, T.R. Sargsyan, *Journal of Physics: Conf. Ser.* **496** (2014) 012009.

[44] G.S. Bisnovatyi-Kogan, *Physical Problems of the Theory of Stellar Evolution*, Moscow, Nauka, 1989. [in russian]

[45] H.S. Zapolsky, E.E. Salpeter, *Astrophys. J.* **158** (1969) 809.

[46] E.E. Salpeter, *Astrophys. J.* **134** (1961) 669.

[47] T. Hamada, E.E. Salpeter, *Astrophys. J.* **134** (1961) 683.

[48] A.Audi et al., *Chin. Phys.* **C36** (2012) 1287.

[49] J.L. Provencal, H.L. Shipman, E.Hog, *Astrophys. J.* **494** (1998) 759.

[50] J.L. Provencal, H.L. Shipman, D. Koester, F. Wesemael, P. Betgeron, *Astrophys. J.* **568** (2002) 324.